Nonlinear low noise particle-in-cell simulations of ETG driven turbulence

A. Bottino, A.G. Peeters, R. Hatzky[2], S. Jolliet[3],

B.F. McMillan[3], T.M. Tran[3] and L. Villard[3]

Max-Planck-Institut für Plasmaphysik,

IPP-EURATOM Association, Garching, Germany

[2] *Computer Center of the IPP and Max-Planck-Gesellschaft, Garching, Germany*

[3] *Centre de Recherches en Physique des Plasmas, EPFL, Lausanne, Switzerland*

(Dated: October 10, 2006)

Abstract

In this letter we show that nonlinear particle-in-cell (PIC) simulations of electron temperature driven turbulence recover the same level of transport as flux-tube codes when the level of statistical noise, associated with the PIC discretisation, is sufficiently small. An efficient measure of the signal-to-noise ratio, applicable to every PIC code, is introduced. This diagnostic provides a direct measure of the quality of PIC simulations and allows for validating analytical estimates of the numerical noise. Global simulations for values of $\rho_e^* < 1/450$ (normalised electron gyroradius) show no evidence of a Gyro-Bohm scaling.

Electron temperature gradient (ETG) driven turbulence may be responsible for the high level of residual electron transport observed in many tokamak internal transport barrier experiments. The linear physics of ETG modes is well known and is similar to that of ion temperature gradient (ITG) modes, with the role of ions and electrons reversed [1]. Therefore, estimates of ETG induced transport based on linear simulations predict diffusion coefficients which are $\sqrt{m_e/m_i}$ smaller as compared to the ITG case. However, ETG and ITG turbulence have a different nonlinear behaviour because of the different adiabatic response of electrons (ITG) and ions (ETG). Quantitative ETG transport predictions made with flux-tube simulations [2, 3] showed that, for certain range of physical parameters, the nonlinear turbulent heat flux can be significantly larger compared to the equivalent ITG case, leading to experimentally relevant levels of radial heat transport ($\chi_e \simeq 13\chi_{gB}$). Such a high transport is attributed to the presence of radially elongated turbulence structures (streamers) and to the consequent $E \times B$ convection. On the other hand, recent global particle-in-cell (PIC) simulations [4, 5] yielded a lower level of anomalous transport as compared to local flux tube Eulerian codes [3]. Radially elongated streamers with width of several ion Larmor radii have been identified but their impact on the transport was found to be small. Although the streamer size scales with the device size, the transport scaling was found to be Gyro-Bohm. Two possible explanations have been proposed to justify this discrepancy: a new nonlinear saturation mechanism associated with toroidal mode coupling [4] and the influence of the non-physical statistical noise due to the particle discretisation [6]. The latter paper shows that in PIC simulations a large level of statistical noise can reduce the ETG turbulence induced transport and can determine the saturation level of the instability.

The purpose of this Letter is to clarify the discrepancy between flux-tube and global PIC results by analysing a set of nonlinear global PIC simulations in which the level of statistical noise is measured and controlled. Results show that low noise PIC simulations produce levels of transport comparable with flux-tube simulations even for relatively large values of $\rho_e^* \equiv \rho_{vth,e}/a$. Here $\rho_{vth,e} = v_{th,e}/\Omega_e$, where $v_{th,e}$ is the electron thermal velocity and Ω_e is the electron cyclotron frequency. The statistical noise has indeed a strong influence on the nonlinear behaviour of ETG turbulence, in agreement with the results of reference [6]. In this letter we also introduce a new measure of the statistical based on a signal-to-noise ratio which provides a direct and trustworthy indicator of the quality of the PIC simulations. We

also show that this diagnostic allows for the validation of analytical estimates for the statistical noise. All the simulations presented in this Letter have been performed with the global gyrokinetic electrostatic code ORB5 [7–9], which uses several techniques of noise reduction, including optimised particle loading [10], Fourier filtering and adaptive gyroaveraging procedure. The code ORB5 solves the gyrokinetic Vlasov equation [11] using marker particles. The projection of the markers on a fixed grid (charge assignment) provides the source term for the quasi-neutrality equation, which is discretised using finite elements (B-splines). Basic physical conservation properties, i.e. energy and particle number, are used as indicators of the quality of the numerical simulations. In all the ETG simulations presented in this work ions are assumed to be adiabatic. Equilibrium n and T_e profiles self-consistently evolve in time, i.e. sources are not included in the simulations. The simulation parameters are basically the CYCLONE case nominal values for the aspect ratio, safety factor and density profile ($R/L_n(r/a \equiv 0.5) = 2.2$) while $\rho_e^* = 1/450, 1/320$ and $1/160$.

Figure 1 shows the temperature gradient evolution (R/L_T) for a $\rho_e^* = 1/450$ circular plasma simulated with 512 million marker particles. The value of R/L_T decreases in time in the region of maximum gradient and increases radially toward plasma edge and centre (radial spreading). Time is measured in $[a/v_{th,e}]$ units and the radial variable is $s \equiv \sqrt{\psi_{\rm pol}}$. The vertical dashed lines in Fig. 1 enclose the radial region in which the temperature gradient exceeds the critical value of the ETG mode (in this case $R/L_{T,\rm crit} \simeq 4.6$) at the end of the simulation. The formation of radially elongated streamers is observed. The radial length of the streamers continuously increases in time following the radial spreading of the temperature gradient and does not appear to converge to a saturation value. Streamers cover the entire radial region where drive is present, i.e. $R/L_T > R/L_{T,\rm crit}$. This is illustrated in Fig. 2, where the dashed flux surfaces correspond to the vertical dashed line in Fig. 1: radially elongated streamers in the electrostatic potential fill the entire radial cross-section where the ETG mode is still unstable, reaching the size of several ρ_i^*. The same behaviour has been observed for all the different values of ρ_e^* used in this work. Therefore, the radial extent of the streamers depends on the choice of the initial temperature gradient profile.

The time evolution of the average value of R/L_T and of the diffusion coefficient χ/χ_{gB} (radial average over $0.52 < s < 0.62$, black vertical lines in Fig. 1) is plotted in black in Fig. 3. During the overshoot the temperature gradient strongly relaxes and falls below the nominal value of the CYCLONE base case $R/L_T = 6.9$. For $t > 80$, R/L_T slowly decays

from $R/L_T \simeq 6.5$ ($\chi/\chi_{gB} \simeq 17$) to $R/L_T \simeq 5.8$ ($\chi/\chi_{gB} \simeq 8.5$). Taking into account that the overshoot strongly depends on the arbitrary initial perturbation, the slowly decaying phase is the only physically relevant part of the simulation. A possible extrapolation for $R/L_T \simeq 6.9$, considering a linear fit of $\chi(R/L_T)$ on the slowly decaying phase only (linear fit for $t > 100$) gives $\chi/(v_{vth,e}\rho_{Te}^2/L_T) \simeq$ [10 to 15] in agreement with the results of flux-tube simulations (more details can be found in Ref. [12]). It is important to notice that in the range $160 < \rho_e^{*-1} < 450$ the scaling of the transport is not gyro-Bohm as it is illustrated in Fig. 3. Therefore, for more realistic values of ρ_e^* the transport induced by ETG turbulence can be even larger than the estimated value for the $\rho_e^* = 1/450$ simulations. Note that in Ref. [4], where a gyro-Bohm scaling of ETG transport was identified, smaller values of ρ_e^* ($500 < \rho_e^{*-1} < 2000$) have been used.

In numerical modelling, in PIC simulations in particular, careful attention must be paid to convergence issues. PIC codes are subject to statistical noise due to the use of marker particles to sample the phase-space. The "statistical noise" is related to the error introduced when moments of the distribution function (for example, the charge assignment) are computed using a finite number of tracers in phase-space [13]. The Monte Carlo theory allows for estimating the contribution of the noise to the charge density ρ:

$$\rho_{\text{noise}}^2 \simeq \frac{N_G}{N_T}\langle w^2\rangle G \quad ; \qquad\qquad \langle w^2\rangle \equiv \frac{1}{N_T}\sum_{i=1}^{N_T} w_i^2 \tag{1}$$

where N_T is the number of tracers, N_G is the number of modes kept in the simulation and w_i is the weight of a single marker. Details about the derivation of Eq. (1) will be given elsewhere. The function G accounts for additional filtering coming through finite Larmor radius effects and the grid projection algorithm. Equation (1) indicates that the statistical noise can be reduced either by increasing the number of tracers ($\sqrt{N_T}$ convergence) or by reducing the number of Fourier modes kept in the simulations (Fourier filtering of non-resonant modes). In addition to this, an important role is played by the control of the evolution of the variance of the distribution of the weights $\sigma \propto \langle w_i^2\rangle$ (optimised loading) [10]. A new diagnostic has been implemented in the code which allows for a direct evaluation of the ρ_{noise}. This measure is based on the average amplitude of the contribution to the charge density, $|\rho_k|$, of the non-resonant (filtered) modes which are physically damped and whose amplitude arises merely from noise. Through the comparison with the charge density of the "physical" modes, a signal to noise ratio can be constructed. This diagnostics provides a direct indicator

of the quality of the numerical simulations during all the time evolution. Moreover, it can be used for validating analytical estimates for the statistical noise like the one proposed in Ref. [6] or the simple estimate of Eq. (1). Several ORB5 simulations showed that the scaling of the noise in the number of particle per mode, N_T/N_G, is in excellent agreement with the estimate of Eq. (1) [12]. Moreover, the scaling of the noise with the number of particles shows that the important parameter in PIC simulations is indeed the number of particle per Fourier mode and not the number of particles per grid cell. A detailed analysis of the scaling of the statistical noise and its impact on physical quantities has been performed and it will be discussed elsewhere. However, it is important to stress the role of the G function: Although the number of numerical particles per mode is a universal scaling for the noise in PIC codes, the scaling factor, i.e. the G function, is strongly algorithm, and therefore code dependent. For example, different projection algorithms in the charge assignment procedure can lead to very different level of noise: Fig. 4 shows that in ORB5 the level of noise is strongly reduced when moving from linear to cubic finite elements. A more detailed analysis shows that linear B-splines require a factor of 4 in the number of particles (for the same number of grid points) as compare to cubic B-splines to obtain the same noise properties.

The effect of the statistical noise on ETG simulations is illustrated in Fig. 5. The statistical noise reduces the level of transport driven by ETG turbulence. Figure 6 shows the noise-to-signal ratio, N/S, for the simulations of Fig. 5: a comparison between Figures 5 and 6 shows that the results start to diverge when the statistical noise becomes larger than 10% of the signal. Note that the slow decaying phase (the only physically relevant phase) disappears and it is replaced by saturated state at very low values of χ/χ_{GB}. This result confirms the predictions of Ref. [6]. When less than 100 particles per mode are used the noise-to-signal ratio is higher than 10% during the entire simulation. In this case even the linear growth rate is not correctly computed. Several tests performed on larger ρ_e^* cases showed in general that $N/S < 10\%$ is required to get converged results, which corresponds to an average value of around 200 markers per mode.

In addition to the reduction of linear drive proposed in Ref. [6], we have observed that the statistical noise creates spurious zonal flows which could contribute to the stabilisation of the turbulence.

We have investigated the role of the nonlinear toroidal coupling of the modes in determining the nonlinear saturation of the turbulence. We have performed a set of flux-tube filtered

simulations in which only a subset of toroidal modes ($n = 0, \pm N, \pm 2N, ...$) are kept in the Poisson equation. These simulations were performed with the same number of markers per mode and show comparable levels of statistical noise. The time evolution of the poloidal wave number spectrum is shown in Fig. 7. The spectrum of the full torus simulation (solid lines) is consistent with the PIC simulations of Ref. [4]. In particular, we observe a nonlinear downshift of the most unstable modes from $0.2 < k_\theta \rho_{Te} < 0.4$ during the linear phase to $0.1 < k_\theta \rho_{Te} < 0.3$ at the end of the simulation. However, flux-tube filtered simulations keeping fixed N_G/N_T do not show significant differences in the downshift of the $k_\theta \rho_{Te}$ spectrum (Fig. 7). The level of transport is slightly higher for a quarter-torus simulation ($N = 4$) as compared to full torus simulations as illustrated in Fig. 8. In conclusion, flux-tube filtered results show an increase of the level of transport as compared to full torus, which is consistent with the predictions of Ref.[4]. However, this effect appears to be small since half torus simulations indeed reproduce the correct level of radial transport for $\rho_e^* = 1/450$. We expect that for even smaller values of ρ_e^*, in which many more toroidal modes are included, computationally costly full torus simulations will not be needed and flux tube filtered simulations (for relatively small values of N) could be used to correctly predict the level of radial transport induced by ETG turbulence.

In summary, global PIC simulations of freely decaying ETG turbulence ($\rho_e^* = 1/450$) show level of transport comparable with flux tube simulations when the statistical noise is sufficiently low. Gyro-Bohm scaling is not observed for $\rho_e^* \leq 1/450$. In global PIC simulations statistical noise reduces ETG driven transport and the level of noise scales with the number of particles per mode but the scaling coefficient strongly depends on the algorithms used in each code. Radially elongated streamers scale with machine size and cover the whole extend of the drive domain. Our flux-tube filtered simulations present a similar spectrum (nonlinear downshift), but (slightly) higher level of transport, as compared to full torus simulations.

Acknowledgment: Simulations were performed on the IBM pSeries Supercomputer "Regatta" of the MPG-IPP Rechenzentrum, Garching, and on the cluster PLEIADES2 of the EPFL, Lausanne.

---

[1] F. Jenko, Comp. Phys. Commun. **125**, 196 (2000).

[2] W. Dorland, F. Jenko, M. Kotschenreuther, and B. Rogers, Phys. Rev. Lett. **85**, 5579 (2000).

[3] F. Jenko and W. Dorland, Phys. Rev. Lett. **89**, 225001 (2002).

[4] Z. Lin, L. Chen, and F. Zonca, Phys. Plasmas **12**, Art. No. 056125 (2005).

[5] Z. Lin, L. Chen, Y. Nishimura *et al.*, Proc. 20th IAEA Fusion Energy Conference 2004, Vilamoura, Portugal, 2004 (IAEA, Vienna, 2005), Paper TH8_4 , (2005).

[6] W.M. Nevins, G.W. Hammett, A.M. Dimits *et al.*, Phys. Plasmas **12**, Art. No. 122305 (2005).

[7] A. Bottino, P. Angelino, S.J. Allfrey *et al.*, *Recent advances in nonlinear gyrokinetic PIC simulations in tokamak geometry* in *Theory of Fusion Plasmas, Int. Workshop* (Editrice Compositori, Societá italiana di Fisica, Bologna, p. 75, 2004).

[8] T. Tran, K. Appert, M. Fivaz, G. Jost, J. Vaclavik, and L. Villard, *Global Gyrokinetic Simulations of Ion-Temperature-Gradient-Driven Instabilities using Paticles* in *Theory of Fusion Plasmas, Int. Workshop, p. 45* (Editrice Compositori, Societá italiana di Fisica, Bologna, 1999).

[9] P. Angelino, A. Bottino, R. Hatzky *et al.*, Phys. Plasmas **13**, 052304 (2006).

[10] R. Hatzky, T. Tran, A. Könies, R. Kleiber, and S. Allfrey, Phys. Plasmas **9**, 898 (2002).

[11] T. Hahm, Phys. Fluids **31**, 2670 (1988).

[12] A. Bottino, A.G. Peeters, R. Hatzky *et al.*, 33rd European Physical Society Conference on Plasma Physics, Rome, June 2006 p. O3.001 (2006).

[13] A. Aydemir, Phys. Plasmas **1**, 822 (1994).

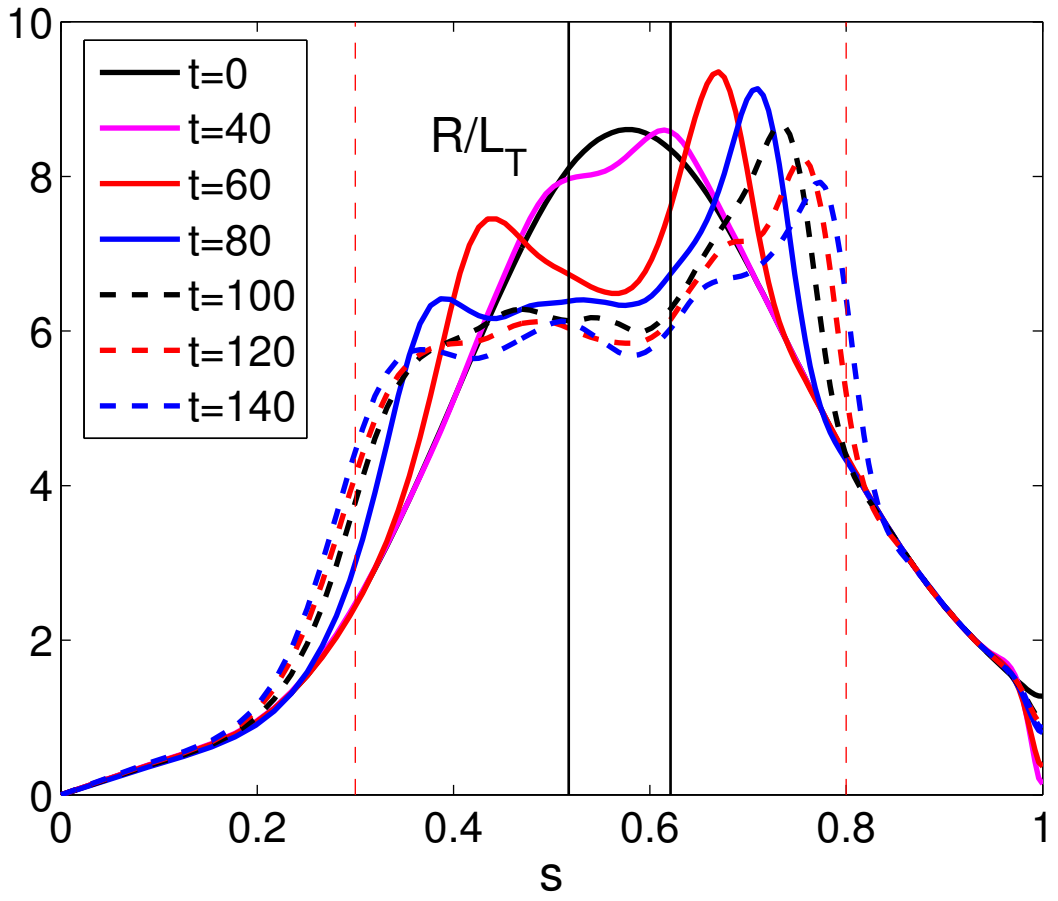

FIG. 1: Evolution of the electron temperature gradient in time $[a/v_{Te}]$. CYCLONE base case, $\rho_e^* = 1/450$, 512 million markers.

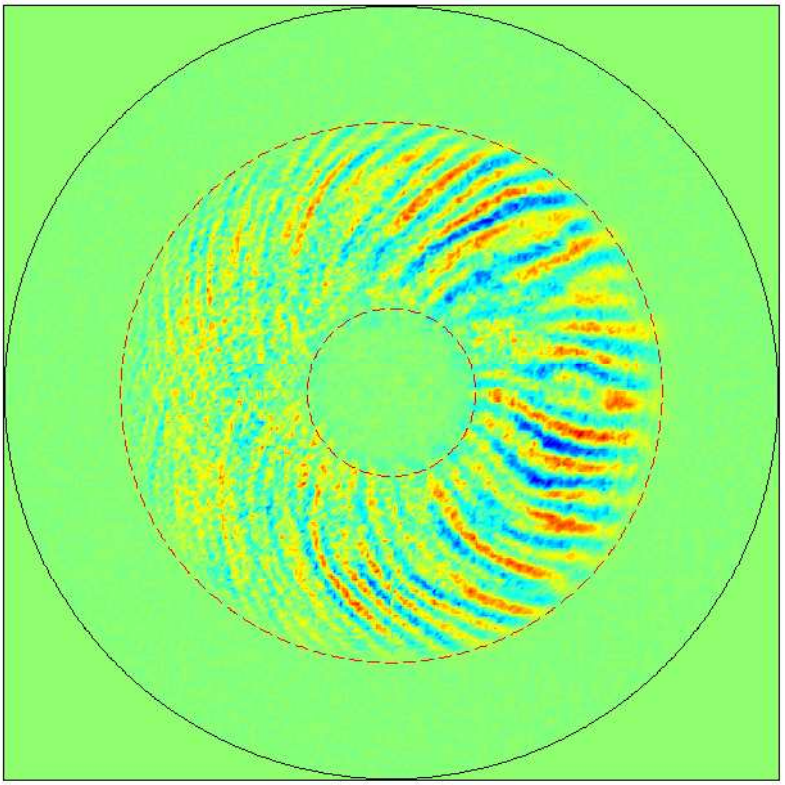

FIG. 2: Cross-section of the lectrostatic potential at $t = 140$ $[a/v_{Te}]$. CYCLONE base case, $\rho_e^* = 1/450$, 512 million markers.

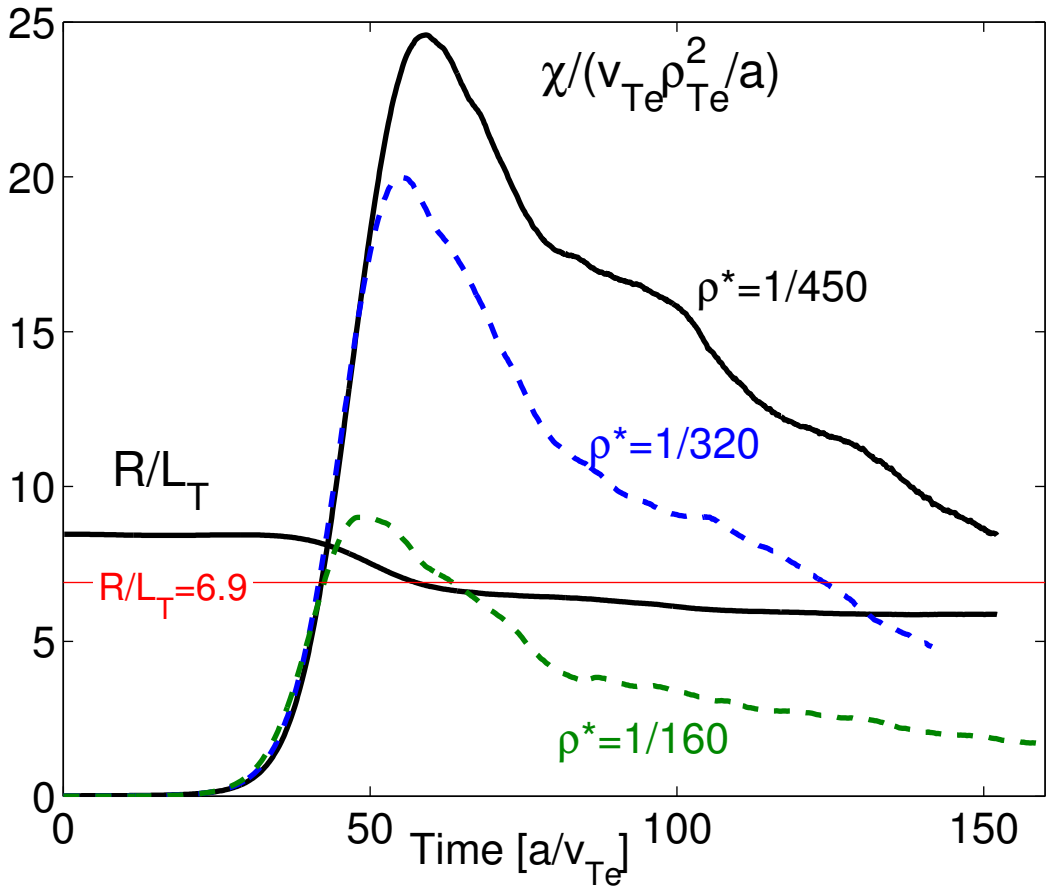

FIG. 3: Time evolution of radial averaged R/L_T and χ/χ_{gB}; radial average over $0.52 < s < 0.62$. CYCLONE base case, $\rho_e^* = 1/450, 1/320, 1/160$. The R/L_T curve plotted here corresponds to the $\rho_e^* = 1/450$ simulation.

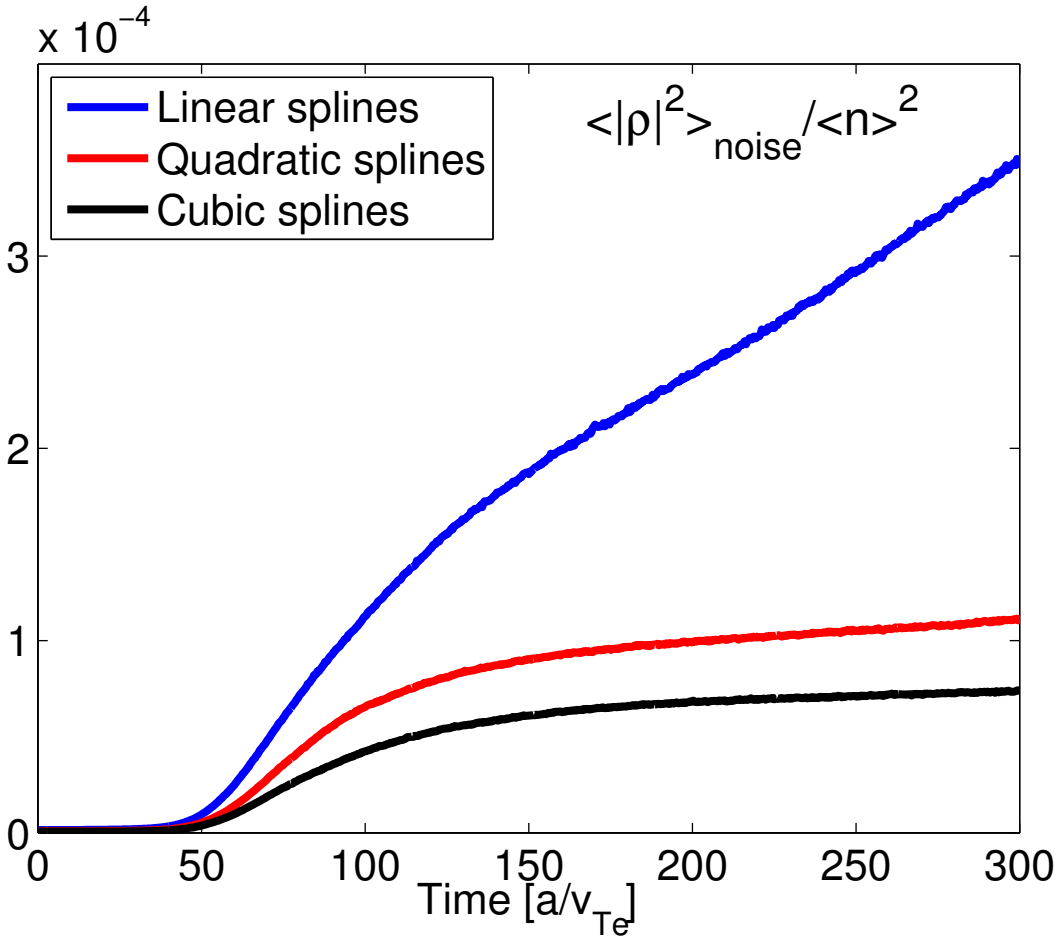

FIG. 4: Scaling of the numerical noise in the charge density with the order of B-splines used in the ORB5 simulations. CYCLONE base case, $\rho_e^* = 1/80$; 64 markers per Fourier mode.

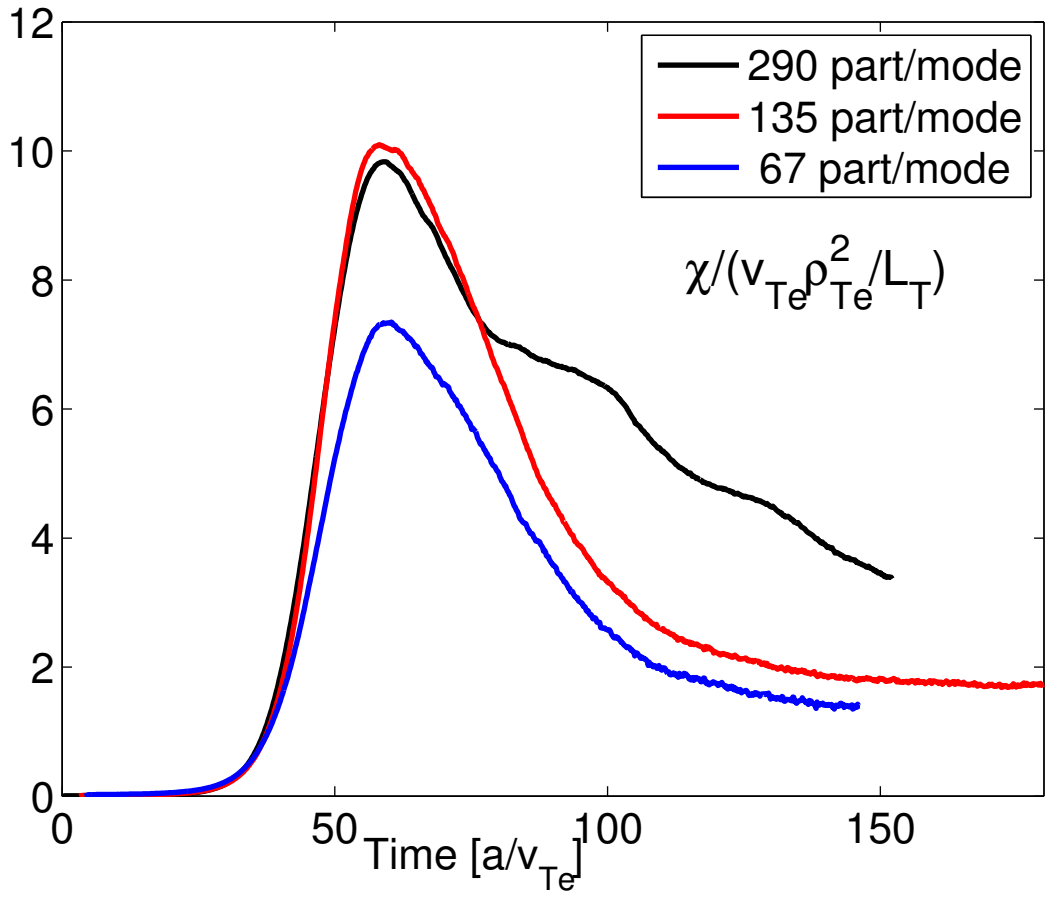

FIG. 5: Time evolution of χ/χ_{gB} and R/L_T for different number of markers per mode (N_T/N_G). CYCLONE base case, $\rho_e^* = 1/450$

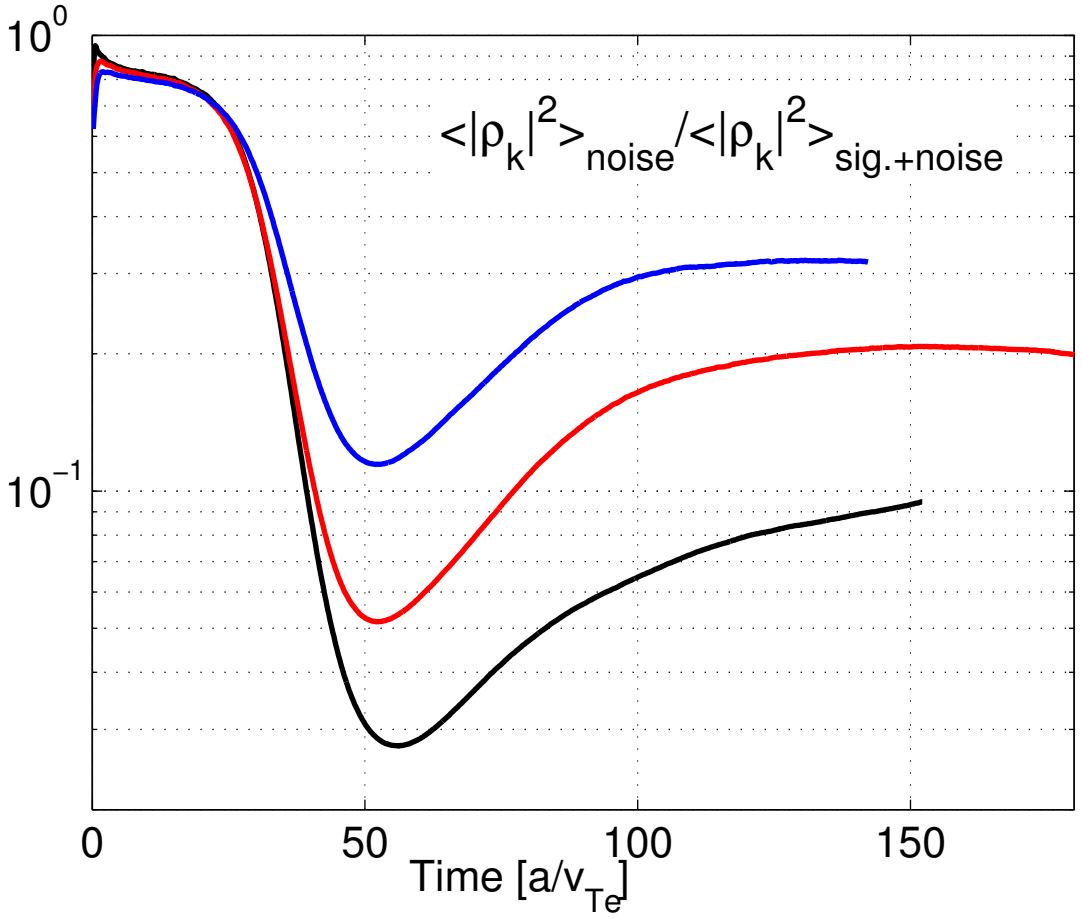

FIG. 6: Noise-to-signal ratio as function of the time for the simulations of Fig. 5. CYCLONE base case, $\rho_e^* = 1/450$, 512 million markers.

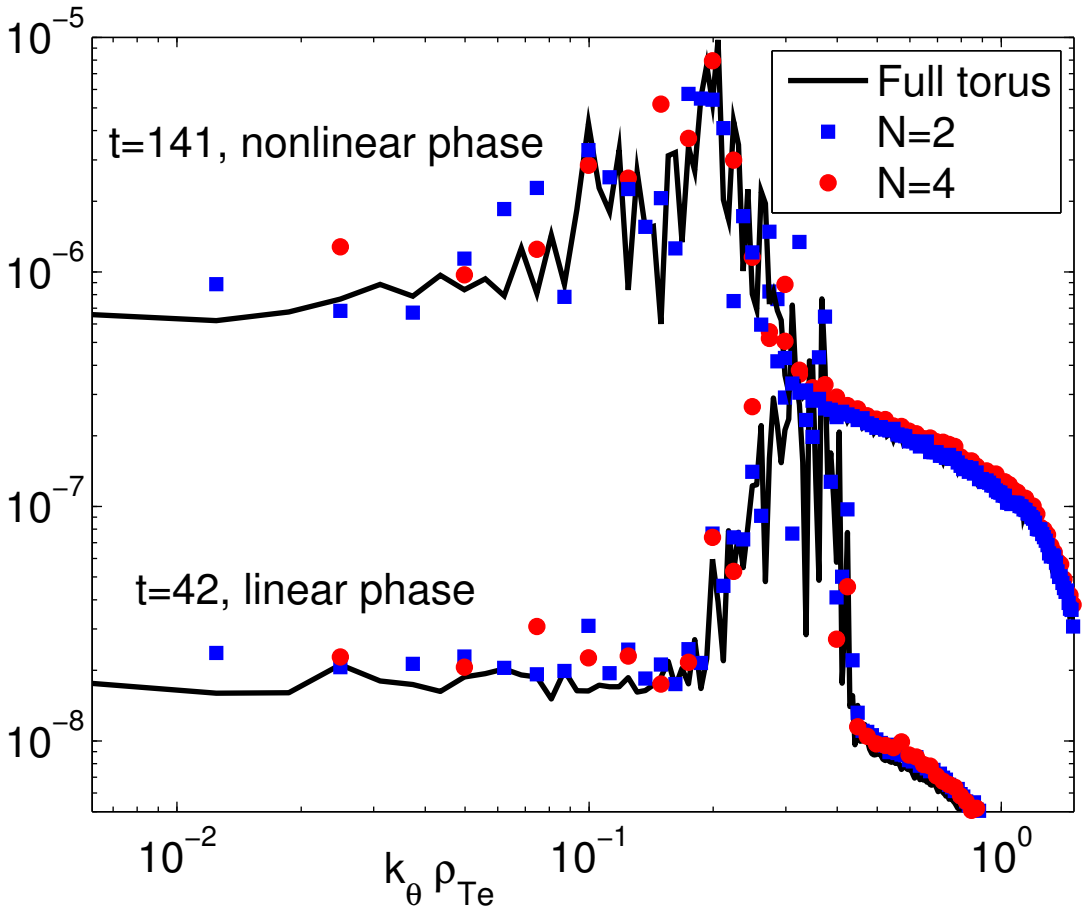

FIG. 7: $k_\theta \rho_e^*$ spectrum or full torus, half torus (N=2) and quarter torus (N=4) flux-tube filtered simulations. CYCLONE base case, $\rho_e^* = 1/450$, number of markers per Fourier mode $N_T/N_G \simeq 290$.

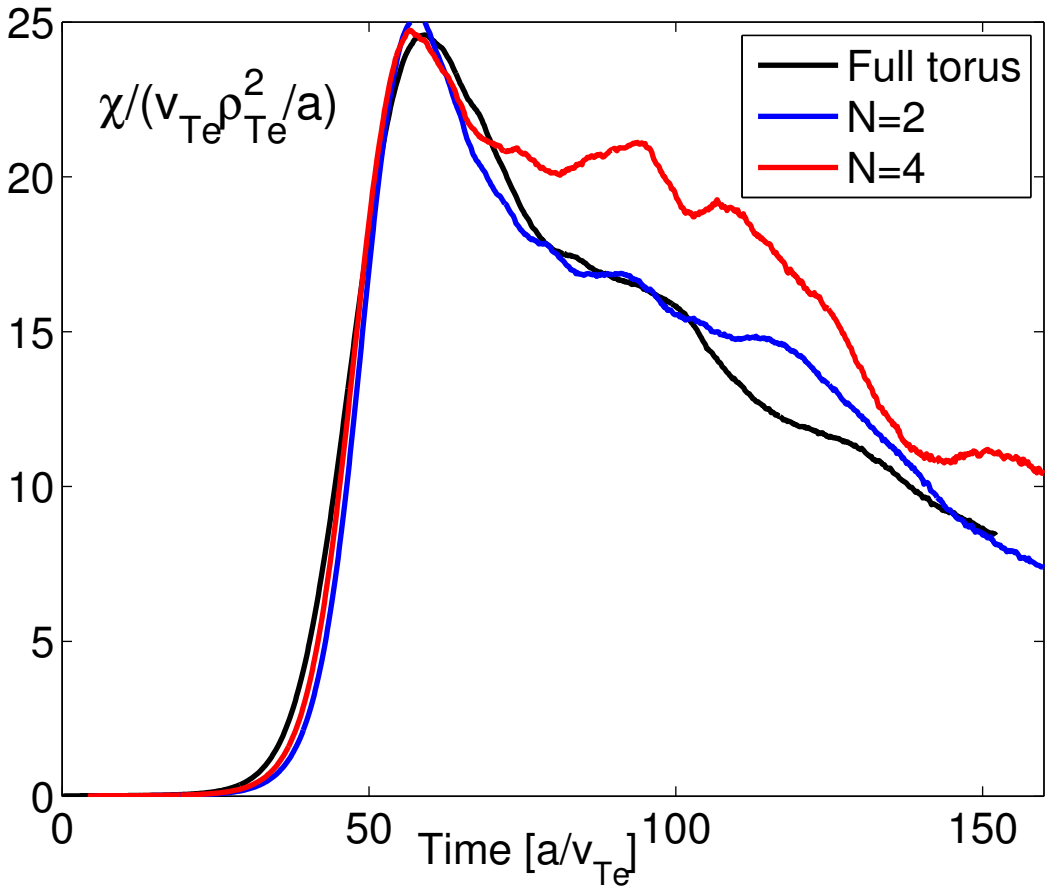

FIG. 8: Time evolution of χ/χ_{gB} full torus, half torus (N=2) and quarter torus (N=4) flux-tube filtered simulations. CYCLONE base case, $\rho_e^* = 1/450$, number of markers per Fourier mode $N_T/N_G \simeq 290$.